WATER RESEARCH 42 (2008) 2269–2277

Available at www.sciencedirect.com

ScienceDirect

journal homepage: www.elsevier.com/locate/watres

Reduction of U(VI) by Fe(II) in the presence of hydrous ferric oxide and hematite: Effects of solid transformation, surface coverage, and humic acid

*Je-Hun Jang**, *Brian A. Dempsey*[1], *William D. Burgos*[2]

Environmental Engineering, The Pennsylvania State University, 212 Sackett Building, University Park, PA 16802, USA

ARTICLE INFO

Article history:
Received 3 August 2007
Received in revised form
27 November 2007
Accepted 6 December 2007
Available online 15 December 2007

Keywords:
U(VI)
Fe(II)
Reduction
Hydrous ferric oxide
Hematite
Mössbauer spectroscopy

ABSTRACT

Fe(II) was added to U(VI)-spiked suspensions of hydrous ferric oxide (HFO) or hematite to compare the redox behaviors of uranium in the presence of two different Fe(III) (oxyhydr)oxides. Experiments were conducted with low or high initial sorption density of U(VI) and in the presence or absence of humic acid (HA). About 80% of U(VI) was reduced within 3 days for low sorbed U(VI) conditions, with either hematite or HFO. The $\{Fe^{3+}\}$ in the low U(VI) experiments at 3 days, based on measured Fe(II) and U(VI) and the assumed presence of amorphous $UO_{2(s)}$, was consistent with control by HFO for either initial Fe(III) (oxyhydr)oxide. After about 1 day, partial re-oxidation to U(VI) was observed in the low sorbed U(VI) experiments in the absence of HA, without equivalent increase of dissolved U(VI). No reduction of U(VI) was observed in the high sorbed U(VI) experiments; it was hypothesized that the reduction required sorption proximity of U(VI) and Fe(II). Addition of 5 mg/L HA slowed the reduction with HFO and had less effect with hematite. Mössbauer spectroscopy (MBS) of ^{57}Fe(II)-enriched samples identified the formation of goethite, hematite, and non-stoichiometric magnetite from HFO, and the formation of HFO, hydrated hematite, and non-stoichiometric magnetite from hematite.

1. Introduction

Reduction of soluble U(VI) by Fe(II) at ambient conditions leads to precipitation of uraninite ($UO_{2(s)}$) or other solid phases. Reduced precipitates of uranium, i.e., with U(IV) or mixed valence, are orders of magnitude less soluble than precipitates of U(VI) (Langmuir, 1978; Missana et al., 2003; Ilton et al., 2005; Renshaw et al., 2005) and their formation results in the immobilization of uranium from contaminated groundwater (Gu et al., 1998). Although reduction of U(VI) by Fe(II) at neutral pH is spontaneous, the reaction is accelerated by Fe(III) (oxyhydr)oxides (Liger et al., 1999; Missana et al., 2003). Reducible metal ions bound to surface hydroxyl groups on the Fe(III) (oxyhydr)oxides are more susceptible to redox reaction due to the changes of electronic structure in the bonding orbitals (Wehrli et al., 1989). In addition, high-resolution X-ray photoelectron spectroscopy revealed that U(V) species formed and were relatively inert on an Fe(II)-rich mica possibly due to polymerization with sorbed U(VI) and U(IV) (Ilton et al., 2005).

Heterogeneous oxidation of Fe(II) with Fe(III) (oxyhydr)oxides occurs with lower activation energy than in homogeneous systems as a function of surface coverage, enhancing the reduction of chemicals such as nitrobenzene (Williams

*Corresponding author. Tel.: +1 814 441 1527; fax: +1 814 863 7304.
E-mail addresses: jhjang2004@gmail.com (J.-H. Jang), bad5@psu.edu (B.A. Dempsey), wdb3@psu.edu (W.D. Burgos).
[1] Tel.: +1 814 865 1226; fax: +1 814 863 7304.
[2] Tel.: +1 814 863 0578; fax: +1 814 863 7304.
0043-1354/$ - see front matter © 2007 Elsevier Ltd. All rights reserved.
doi:10.1016/j.watres.2007.12.007

and Scherer, 2004), CCl_4 (Amonette et al., 2000), and O_2 (Park and Dempsey, 2005). However, the Fe(II)-driven reduction of contaminants coupled with pre-formed Fe(III) (oxyhydr)oxides can be easily complicated by the solid-phase transformations that produce new Fe(III) (oxyhydr)oxide phases during the reduction, due to electron transfer (Tronc et al., 1992; Williams and Scherer, 2004; Larese-Casanova and Scherer, 2007) or dissolution followed by reprecipitation (Feitknecht and Michaelis, 1962; Jang et al., 2003; Pedersen et al., 2005). Pedersen et al. (2005) reported release of "congruently incorporated" ^{55}Fe from hydrous ferric oxide (HFO), lepidocrocite, and goethite upon contact with Fe(II). The release of ^{55}Fe from HFO was followed by partial conversion to lepidocrocite and goethite, consistent with the earlier postulate that the Fe(II) can induce dissolution of the pre-formed Fe(III) (oxyhydr)oxides followed by re-precipitation (Feitknecht and Michaelis, 1962). Tronc et al. (1992) observed the formation of spinel from Fe(II)–HFO experiments. Scherer and co-workers showed that the electrons can be exchanged between sorbed Fe(II) and underlying Fe(III) (oxyhydr)oxides, resulting in the formation of epitaxial layers (Williams and Scherer, 2004; Larese-Casanova and Scherer, 2007). Non-stoichiometric (NS) magnetite (indicative of internal electron transfer) plus goethite was formed when Cu^{2+} or NO_3^- (both oxidizers) were added to Fe(II)-spiked HFO (Jang et al., 2003).

Therefore, characterization of the solids after reaction with Fe(II) is important when assessing the mechanisms of Fe(II)-driven U(VI) reduction. Similarly, the Nernstian reduction potential of an Fe(II)–Fe(III) system is determined by $\{Fe^{3+}\}$, i.e., by the solubility of Fe(III) (oxyhydr)oxides (Stumm and Morgan, 1996). Thus, mineralogical changes could result in changing reduction potentials in Fe(II)–Fe(III) systems.

Many Fe(II)–Fe(III) systems, where the formation of new phase or transformation were not investigated, have documented discrepancies between measured and theoretical reduction potentials. Liger et al. (1999) reported rapid (the reaction mostly occurred within the first hour) but less than theoretical reduction of U(VI) by Fe(II) with hematite. They suggested that the incomplete reduction was due to the formation of U(VI) surface precipitates or mixed valence uranium oxides that inhibited the electron transfer from Fe(II) to U(VI). Measured reduction potentials for Fe(II) and goethite or lepidocrocite were higher (less reducing) than predicted based on solubilities of the bulk phases (Macalady et al., 1990; Silvester et al., 2005) and, sometimes, were in agreement with solubility predictions for HFO (Grenthe et al., 1992; Silvester et al., 2005). Other anomalies have been observed; for example, the potential measured during bioreduction of HFO and goethite first decreased, then increased, and finally decreased again to a lower potential (Petruzzelli et al., 2005). These anomalies have sometimes been attributed to poor electrochemical equilibration with the electrode (Morris and Stumm, 1967; Lindberg and Runnells, 1984; Silvester et al., 2005).

In this study, we investigated the kinetics of Fe(II)-driven reduction of U(VI) as functions of mineralogy of the initial Fe(III) (oxyhydr)oxides (HFO or hematite), initial U(VI) surface coverage, and humic acid (HA). HAs are ubiquitous in natural environments and can catalyze and participate in redox reactions (Voelker et al., 1997). HFO and hematite were selected as starting phases due to the large difference in thermodynamic solubility (NIST, 2004), hence, in the theoretical reduction potentials for the Fe(II)–Fe(III) system. Mineralogical changes in HFO and hematite were monitored using ^{57}Fe-Mössbauer spectroscopy (MBS).

2. Materials and methods

All chemicals were of reagent grade or higher. Aldrich® HA was rehydrated for at least 24 h at pH >10. We used distilled water to produce deionized (DI) water, which was also filtered twice through 0.2 μm filters to exclude bacterial contamination. Solid reagents and DI water were stored, solutions and suspensions were prepared, and experiments were run in an anoxic glove bag (97:3 N_2:H_2 mixture with Pd catalyst and gas monitor) with bag gas continuously recycled through an "O_2 scavenger" (3.3 mM $FeCl_2$, 6.6 mM $FeCl_3$, 0.1 M $NaNO_3$, and pH 8.4, Tamura et al., 1976). Experiments were started after at least 2 days of O_2 scavenging. These precautions were essential; the concentration of HCl-extractable Fe(II) in the O_2-scavenger suspension decreased during 2 days after using the interlock and then stabilized. The gas monitor showed "zero ppm O_2" for the 2 days, indicating that trace level of oxygen that can oxidize aqueous Fe(II) lingered for 2 days not being detected by the gas monitor. Bag gas was dehumidified and was exposed to NaOH pellets to remove CO_2.

The U(VI) reduction experiments were initiated by adding Fe(II) (0.1mM) to the HFO and hematite suspensions (1mM as Fe(III), 0.01 M NaCl). Syntheses and descriptions of HFO and hematite are in Jang et al. (2007a). The Fe(II) stock was prepared by dissolving standard iron wire in dilute HCl and was enriched with ^{57}Fe(II) (50%) to improve detection with MBS. U(VI) and HA (for some experiments) were added just before the addition of Fe(II). The pH was adjusted to 6.8 with HCl or NaOH. For "low-ΣU" experiments, 4.5 and 1 μM U(VI) were added to HFO and hematite suspensions, respectively, producing sorption densities of 0.055(±0.006) U(VI)/nm^2. For "high-ΣU" experiments, 45 and 10 μM U(VI) were added to produce 0.55(±0.06) U(VI)/nm^2 (Jang et al., 2007a).

Reduction from U(VI) to U(IV) was determined by the decrease in extracted U(VI) (0.17 M H_3PO_4). Phosphoric acid is an efficient extractant for solid-associated U and was used instead of carbonate solutions in order to avoid contamination of the glove bag with CO_2. Dissolved U(VI) in filtrate (0.1 μm syringe filter) and extracted U(VI) samples were analyzed by the Kinetic Phosphorescence Analyzer (KPA, ChemChek, Inc.). The KPA is sensitive only to U(VI). Phosphate up to 10 mM in analytical samples did not interfere (Sowder et al., 1998). A test was performed to see whether phosphoric acid extracts both U(VI) and U(IV); some aliquots of extraction samples were exposed to normal atmosphere for up to 36 h. We observed that [U(VI)] in the phosphoric acid extraction increased more than 60% of initially added [U(VI)] upon exposure to air, confirming that the reduction occurred.

Therefore, samples and calibration standards were combined with deoxygenated Uraplex®[3] in plastic syringes while

[3] U(VI) complexant for stable laser-induced phosphorescence in KPA analysis. Patented material by ChemChek, Inc.

still inside the glove bag. Syringe tips were sealed with rubber caps, syringes were removed from glove bag, and the contents injected directly into the KPA phosphorescence cell while flushing the previous samples, avoiding any contact with air. Some aliquots of filtrates were oxidized with H_2O_2, but no increase of "$[U(VI)_{diss}]$" was observed, indicating that all U(IV) was removed by membrane filtration due to precipitation and sorption. Fe(II) was measured using phenanthroline for dissolved and 0.1 M HCl-extractable Fe(II), using fluoride as a masking reagent for Fe(III) in the HCl-extracted Fe(II) samples (Tamura et al., 1974).

Transmission ^{57}Fe-MBS was used at room temperature to characterize Fe(III) (oxyhydr)oxides before and after the reduction. ^{57}Fe-MBS is more sensitive to minority phases (Murad, 1990) and long-range crystalline arrays are not as essential as for analysis with X-ray diffraction. A ^{57}Co/Rh source of 25 mCi initial activity was used. The source velocity was kept between $\pm$12 mm/s using constant acceleration mode, with a 1024 pulse-height analyzer recording the signals. Recorded spectra were calibrated with respect to standard iron foil. Commercial hematite (Fisher®) and magnetite (Alfa-aesar®), used as standards, had Mössbauer parameters in agreement with the literature (Cornell and Schwertmann, 1996).

The computer program "*Recoil*" (Lagarec and Rancourt, 1998) was used to analyze the Mössbauer spectra. Lorentzian line-shape analysis was applied for individual minerals. Half-width at half maximum (HWHM) was typically less than 0.15 mm/s for individual peaks that were used to deconvolute the superposed peaks. Peaks with HWHM more than 0.15 mm/s were attributed to distribution of hyperfine magnetic fields (H in kOe) due to poly-disperse particle sizes, poor crystallinity, or NS precipitates (Murad, 1982; Murad and Schwertmann, 1993). The Voigt-based fitting (VBF) procedure was used to determine the distribution of *H* values (Rancourt and Ping, 1991; Lagarec and Rancourt, 1998).

3. Results and discussion

3.1. *Reduction and sorption of U(VI)*

Reduction of U(VI) by Fe(II) in the presence of HFO or hematite in the low-Σ*U* experiments is illustrated in Fig. 1 (solid symbols); we did not observe any reaction in our high-Σ*U* experiments (open symbols). Liger et al. (1999) conducted experiments using hematite with nearly identical sorption density of U(VI) and Fe(II) as in our low-Σ*U* experiments. Their results (× , Fig. 1a) were very similar to our results; the initial fast reduction was followed by slower reduction, and the extent of reduction was less than the thermodynamic prediction.

The initial rate of reduction of U(VI) in the low-Σ*U* experiments was faster with hematite than with HFO (Fig. 1a), but the final extent of reduction was similar (82% with HFO and 76% with hematite). The different initial reduction rates may be explained by the presence of hematite versus HFO. Whereas, the similar final extents of reduction in the two experiments may indicate convergence of Fe(III) (oxyhydr)oxide reaction products (see Section 3.2 for discussion on $\{Fe^{3+}\}$). Lower initial solubility of the Fe(III) (oxyhydr)-oxide phase in the hematite experiments results in a more reducing Nernstian potential and is consistent with a greater driving force for reaction.

There was no reduction of U(VI) in the high-Σ*U* experiments (open symbols, Fig. 1), which is counter-intuitive; one might expect a greater driving force with higher concentration of sorbed U(VI). We also observed decreased rate of redox reaction with increasing surface coverage for Fe(II)/O_2 (Park and Dempsey, 2005) and for Fe(II)/NO_2^- (our current work in progress), both reactions catalyzed by HFO. We hypothesized a need for propinquity of reactive surface sites at which oxidation and reduction can occur, i.e., high surface coverage

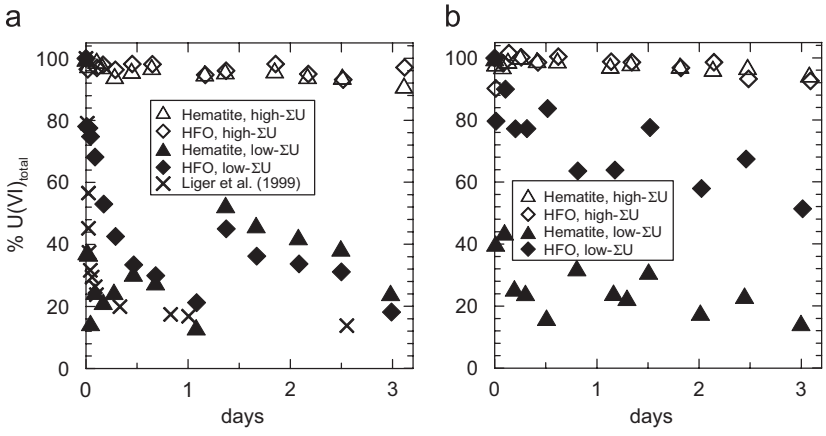

Fig. 1 – Reduction of U(VI) by Fe(II) at pH 6.8 in "low-Σ*U*" (solid symbols) and "high-Σ*U*" (open symbols) experiments (a) in the absence of and (b) with 5 mg/L humic acid. Σ*U* represents total added uranium as U(VI). The concentrations of HFO and hematite were 1 mM as Fe(III) for this study. The initial surface coverage was 0.055($\pm$0.006) and 0.55($\pm$0.06) U(VI)/nm^2 in low- and high-Σ*U* experiments, respectively. Liger et al. (1999) (cross symbols) reported similar results with initial surface coverage of 0.02 U(VI)/nm^2 at pH 7.5.

of one sorbate could decrease the probability of finding both anodic and cathodic sites within a reactive distance on the surface (Park and Dempsey, 2005).

Addition of HA decreased the extent of reduction of U(VI) in the presence of HFO and slightly increased the extent of reduction in the presence of hematite in the low-ΣU experiments (solid symbols, Fig. 1b). HA could have several effects on the redox reaction; HA sorbs on HFO and hematite (Tipping, 1981), forms dissolved complexes with Fe(III) and U(VI) (Tipping et al., 2002), increases the sorption of U(VI) onto ferric (oxyhydr)oxides (Ho and Miller, 1985; Payne et al., 1996; Lenhart and Honeyman, 1999), and can catalyze or hinder redox reactions (Voelker et al., 1997). HA can modify the stability and surface reactivity of HFO (Weber et al., 2006), and can inhibit transformation to more stable phases (Schwertmann, 1966). Addition of HA did not affect total residual U(VI) in the high-ΣU experiment (open symbols, Fig. 1b), i.e. there still was no measurable reduction.

Dissolved U(VI) concentration ($[U(VI)_{diss}]$) was nearly invariant after 0.5 days (Fig. 2) despite variation in $[U(VI)_{total}]$ with time (solid symbols, Fig. 1). Most residual U(VI) was sorbed. We previously reported conditions that result in precipitation of U(VI) for higher $[U(VI)_{diss}]$ (Jang et al., 2006). There was no increase in $[U(VI)_{diss}]$ in the filtrates after oxidation with H_2O_2, indicating negligible passage of U(IV) through the membrane filters. Overall, more than 96% of initial U(VI) was removed from the aqueous phase by sorption and reductive precipitation in the low-ΣU experiments. In high-ΣU experiment where the reduction was insignificant, complete removal of uranium was attributed to sorption and HA enhanced sorptive removal (Fig. 2).

The concentrations of sorbed and dissolved Fe(II) were nearly constant within error during the experiment (Fig. 3); 82(±4)% stayed in aqueous phase and 95(±4)% of added Fe(II) was extracted. Based on the final $[U(VI)_{total}]$ in the low-ΣU experiment (Fig. 1), we expected 93% of added Fe(II) to be present at the end of the experiment.

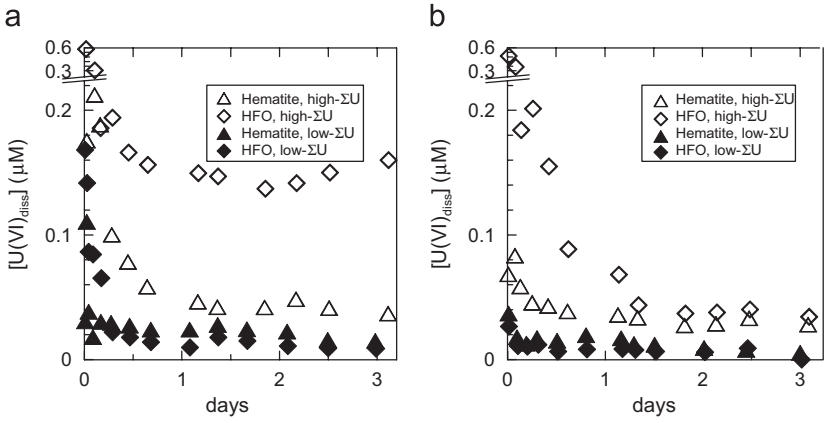

Fig. 2 – $[U(VI)_{diss}]$ during the reduction (a) without HA and (b) with 5 mg/L HA. $[U(VI)_{diss}]$ was undersaturated with respect to schoepite (Langmuir, 1978; Jang et al., 2006) throughout the experiments, indicating that $[U(VI)_{diss}]$ was controlled by sorption onto HFO or hematite.

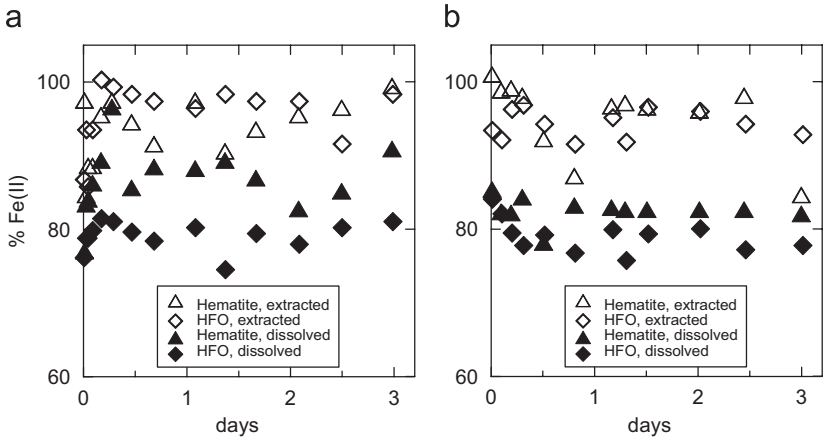

Fig. 3 – Dissolved and extracted Fe(II) concentrations during "low-ΣU" experiments with (a) 0 and (b) 5 mg/L humic acid. Initial concentration of Fe(II) was 100 μM. On average, 95(±4)% of added Fe(II) was extracted and 82(±4)% was dissolved. Based on the measured reduction of U(VI) to U(IV), 93% of Fe(II) should have been available for extraction.

We observed partial re-oxidation of uranium after 0.1 days for hematite and after 1.3 days for both HFO and hematite (Fig. 1a), although there was no significant increase in $[U(VI)_{diss}]$ (Fig. 2). We believe that this study is the first report on the Fe(II)-driven U(VI) reduction for the time interval of 1.0–2.5 days that included measurements of dissolved U(VI) and Fe(II). Experimental anomalies are unlikely; the interlock was not used, no other experiments were simultaneously conducted, and O_2 was not admitted based on the O_2 monitor and no further loss of Fe(II) in the O_2 scavenger.

Though the mechanism of the partial re-oxidation is unclear from this study, observations of oscillating concentrations of reduced or oxidized species and oscillating redox potential during bioreduction of HFO and goethite have been reported by others (Petruzzelli et al., 2005). This could be due to slow structural reorganization of reduced and oxidized precipitates (Grenthe et al., 1992), e.g., conversion to more stable Fe(III)(hydr)oxide resulting in decreased $\{Fe^{3+}\}$ (Stumm, 1992), which, in turn, can result in oscillation of reduction potentials. Grenthe et al. (1992) reported that ~24 h were required to obtain a stable redox potential in the Fe(II)–HFO system due to slow recrystallization of HFO. A sudden change in the concentration of total U(VI) could also be due to disproportionation of U(V) that was precipitated or sorbed, and thus not available for extraction and analysis under the conditions of our experiments and analyses. U(V) has been shown to be meta-stable when sorbed (Ilton et al., 2005). Disproportionation, resulting in oscillating redox potential, has been observed for other elements, e.g, arsenic (Stauder et al., 2005) and manganese (Postma and Appelo, 2000). The formation of a mixed valence precipitate such as $U_3O_{8(s)}$ seems unlikely in this case, since precipitation of $U_3O_{8(s)}$ should have resulted in significantly lower $[U(VI)_{diss}]$ than observed.

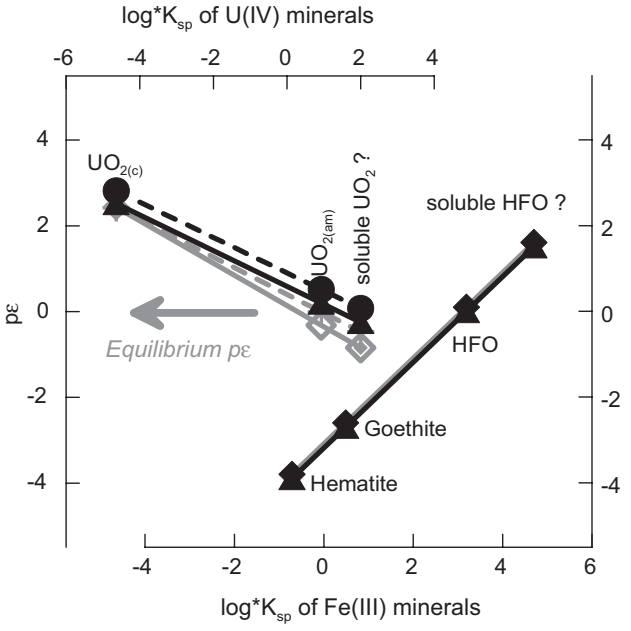

Fig. 4 – Redox $p\varepsilon$ values based on final $[U(VI)_{diss}]$ and $[Fe(II)_{diss}]$ (pH 6.8, $I = 0.01$ as NaCl) and reactions in Table 1. Left y-axis for U(IV)/U(VI) half reactions: gray lines for "low-ΣU", black lines for "high-ΣU" experiments, and dashed lines for experiments with humic acid (HA). Right y-axis for Fe(II)/Fe(III) half reactions: gray line for "low-ΣU", and black line for "high-ΣU" experiment. The $p\varepsilon$ values for Fe(II)/Fe(III) did not change with addition of HA. Small fluctuations in solubility of Fe(III) minerals during aging process (i.e., dissolution and reprecipitation) could result in temporal, partial re-oxidation of uranium.

3.2. *Thermodynamic analysis*

The $p\varepsilon$ values of half reactions depend on $\{Fe^{3+}\}$ and associated solid phase with Fe(III), and $\{U^{4+}\}$ and associated solid phase with U(IV). The $p\varepsilon$ values of the half reactions involving those two elements should be identical when the system is at equilibrium (Appelo and Postma, 1993). Redox ladders for possible half reactions are illustrated as a function of solubility products of possible minerals for Fe(III) and U(IV)

Table 1 – Reactions used to predict speciation and equilibrium $p\varepsilon$ of the half reactions

Reactions	*K*
Uranium	
$UO_2^{2+}+4H^++2e^- \Leftrightarrow U^{4+}+2H_2O$	$10^{9.22}$
$UO_{2(c)}+4H^+ \Leftrightarrow U^{4+}+2H_2O$: crystalline uraninite	$10^{-4.64}$
$UO_{2(am)}+4H^+ \Leftrightarrow U^{4+}+2H_2O$: amorphous uraninite	$10^{0.93}$
$U_3O_8+4e^-+16H^+ \Leftrightarrow 3U^{4+}+8H_2O$: mixed valence solid	$10^{21.11}$
$U^{4+}+H_2O \Leftrightarrow UOH^{3+}+H^+$	$10^{-0.65}$
$U^{4+}+2H_2O \Leftrightarrow U(OH)_2^{2+}+2H^+$	$10^{-2.25}$
$U^{4+}+3H_2O \Leftrightarrow U(OH)_3^{1+}+3H^+$	$10^{-4.89}$
$U^{4+}+4H_2O \Leftrightarrow U(OH)_4^{0}+4H^+$	$10^{-8.54}$
$U^{4+}+5H_2O \Leftrightarrow U(OH)_5^{1-}+5H^+$	$10^{-13.16}$
$6U^{4+}+15H_2O \Leftrightarrow U_6(OH)_{15}^{9+}+15H^+$	$10^{-17.22}$
$UO_2(OH)_2 \cdot H_2O+2H^+ \Leftrightarrow UO_2^{2+}+3H_2O$: hydrated schoepite	$10^{5.39}$
$UO_2^{2+}+H_2O \Leftrightarrow UO_2OH^++H^+$	$10^{-5.78}$
$2UO_2^{2+}+2H_2O \Leftrightarrow (UO_2)_2(OH)_2^{2+}+2H^+$	$10^{-5.62}$
$3UO_2^{2+}+5H_2O \Leftrightarrow (UO_2)_3(OH)_5^{+}+5H^+$	$10^{-5.78}$
Iron	
$Fe^{3+}+e^- \Leftrightarrow Fe^{2+}$	$10^{13.0}$
$(1/2)\alpha\text{-}Fe_2O_3+3H^+ \Leftrightarrow Fe^{3+}+(3/2)H_2O$: hematite	$10^{-0.71}$
α-FeOOH$+3H^+ \Leftrightarrow Fe^{3+}+2H_2O$: goethite	$10^{0.49}$
$Fe(OH)_{3(am)}+3H^+ \Leftrightarrow Fe^{3+}+3H_2O$: HFO	$10^{3.19-4.70}$
$Fe(OH)_{2(am)}+2H^+ \Leftrightarrow Fe^{2+}+2H_2O$	$10^{13.5}$
$Fe_3O_{4\ (c)}+8H^+ \Leftrightarrow Fe^{2+}+2Fe^{3+}+4H_2O$: magnetite	$10^{3.40}$
$Fe^{2+}+H_2O \Leftrightarrow FeOH^++H^+$	$10^{-9.4}$
$Fe^{2+}+2H_2O \Leftrightarrow Fe(OH)_2^{0}+2H^+$	$10^{-20.6}$
$Fe^{2+}+3H_2O \Leftrightarrow Fe(OH)_3^{1-}+3H^+$	$10^{-31.0}$
$Fe^{3+}+H_2O \Leftrightarrow FeOH^{2+}+H^+$	$10^{-2.19}$
$Fe^{3+}+2H_2O \Leftrightarrow Fe(OH)_2^{1+}+2H^+$	$10^{-4.59}$
$Fe^{3+}+4H_2O \Leftrightarrow Fe(OH)_4^{1-}+4H^+$	$10^{-21.59}$
$2Fe^{3+}+2H_2O \Leftrightarrow Fe_2(OH)_2^{4+}+2H^+$	$10^{-2.85}$
$3Fe^{3+}+4H_2O \Leftrightarrow Fe_3(OH)_4^{5+}+4H^+$	$10^{-6.29}$

All *K*'s are for I = 0. The equilibrium constants for Fe are from NIST (2004), *U* from Langmuir (1978). Redox potentials were defined as "reduction", solubilities were defined as "dissolution involving H^+", and hydrolysis reactions were cumulative ones with cations (Fe^{2+}, Fe^{3+}, or UO_2^{2+}) and H^+.

(Fig. 4). Potentials were calculated using reactions in Table 1, experimental data, and Visual MINTEQ (Gustafsson, 2006) was used to calculate activities of pertinent species. Each line represents different experimental conditions. Schoepite was always undersaturated during the experiments (Langmuir, 1978; Jang et al., 2006). Based on these calculations, HFO and amorphous uraninite ($UO_{2(am)}$) were the most likely phases controlling redox potential.

More soluble HFO phases have been reported as reaction intermediates. $^{*}K_{sp}$ values for HFO as high as $10^{4.70}$ have been measured during oxidation of Fe(II) and has been attributed to more OH-bridged Fe^{3+} in the structure (Langmuir and Whittemore, 1971; Grenthe et al., 1992). This indicates that higher reducing potentials can be intermittently posed due to higher $\{Fe^{3+}\}$ as the reaction approaches equilibrium. HA can also affect the solubility of HFO. Weber et al. (2006) reported very high $^{*}K_{sp}$ for HFO ($10^{5.6–5.7}$) for the Fe(III)–HA system, attributed to incorporation of HA as a co-ligand (Allard et al., 2004).

3.3. *Fe(III) (oxyhydr)oxides phase changes*

MBS indicated that substantial phase transformations occurred in Fe(III) (oxyhydr)oxides for either the HFO or hematite experiments (Fig. 5 and Table 2). Only 3.4% and 6.0% of initial HFO and hematite left after 3 days. Goethite, hematite, and NS magnetite were formed from HFO (Fig. 5b). HFO, along with other phases, was produced in the hematite experiments as well (Fig. 5d). NS goethite (Murad, 1982; Jang et al., 2003) was the dominant phase (53.9%) discovered in the HFO experiments and hydrated hematite (Jang et al., 2007b) was the dominant phase (61.5%) in hematite experiments,

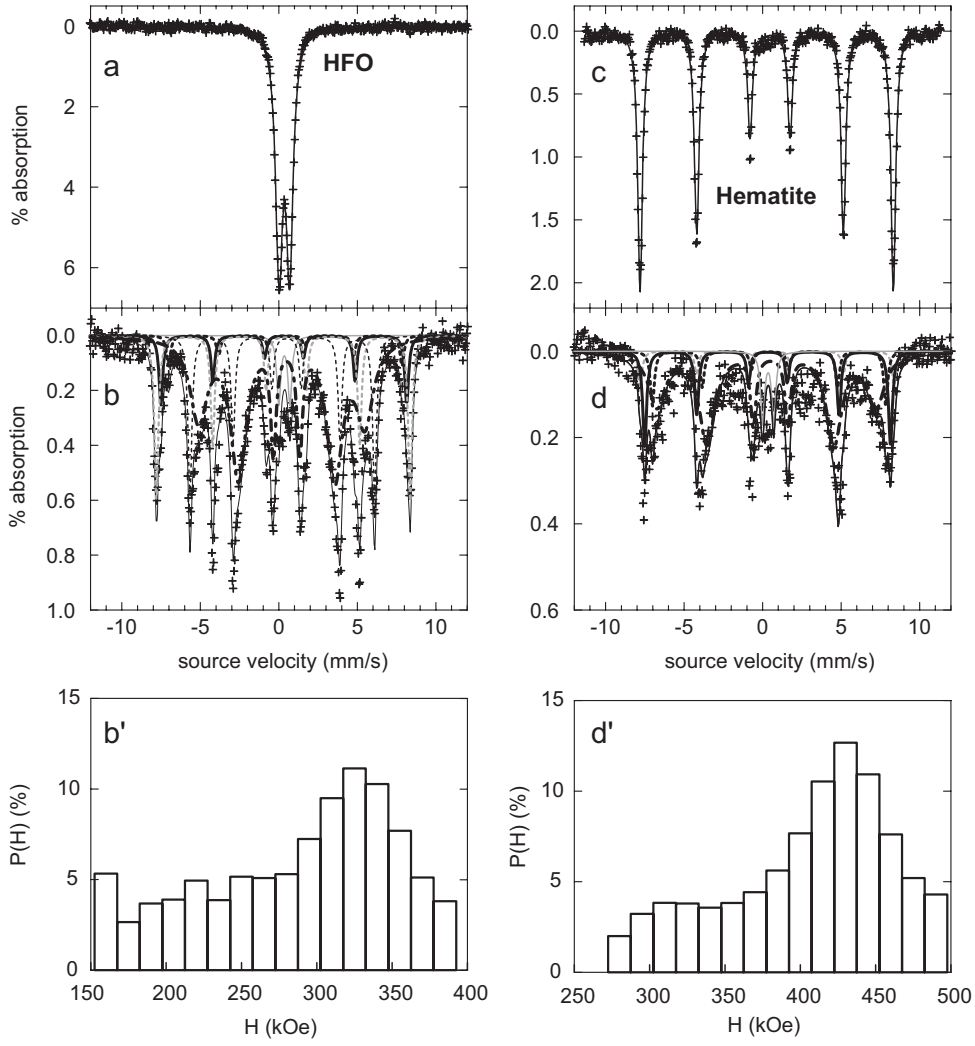

Fig. 5 – Mössbauer spectroscopy analysis of solids from "low-ΣU" experiments without humic acid: (a) and (b) are HFO before and after the experiment; (c) and (d) are hematite before and after the experiment. In (b) and (d), HFO (central thin gray solid line), hematite (thick gray dotted line), non-stoichiometric magnetite (thick black solid and black dotted line for tetrahedral and octahedral sites, respectively) were present. (b′) and (d′) show distributions of the hyperfine magnetic fields (H in kOe) for NS goethite (Murad, 1982; Jang et al., 2003) in (b) and hydrated hematite (Jang et al., 2007b) in (d) (both described using thickest dash-dot lines). Relative areas of individual peaks and Mössbauer parameters are listed in Table 2.

Table 2 – Peak area analysis of Mössbauer spectra (Figs. 5b and d)

Initial solids		% Peak area HFO	% Peak area Hematite	Fe valency	CS[a] (mm/s)	QS[b] (mm/s)	H^c (kOe)
Solids in product							
HFO		3.4	6.2	Fe(III)	0.35	0.71	
Hematite		16.7	6.0	Fe(III)	0.38	−0.09	501[d]
NS[e]-magnetite	Th[f]	6.9	16.7	Fe(III)	0.33	−0.01	485
	Oh[g]	3.1	9.6	*Fe(II)*[h]	0.44	−0.03	461
Goethite		16.0	–	Fe(III)	0.36	−0.14	365
NS-goethite		53.9	–	Fe(III)	–	–	–
Hydrated hematite		–	61.5	Fe(III)	–	–	–

[a] Center shift.
[b] Quadrupole splitting.
[c] Hyperfine magnetic field.
[d] *H* for hematite of sub-μm diameter ranges 506–515 kOe (Hobson and Gager, 1970). *H* values lower than this range may indicate hydration of hematite that results in reduced hyperfine magnetic fields (Jang et al., 2007b).
[e] Non-stoichiometric (Murad, 1982).
[f] Tetrahedral site in magnetite.
[g] Octahedral site in magnetite.
[h] Maximum concentration of Fe(II) (in italic).

shown by the black dash dot lines in Fig. 5b and d. Crystalline hematite also showed reduced *H* values (501 kOe, Table 2), probably due to hydration. Those sub-spectra were analyzed using the VBF procedure to determine the distribution of hyperfine magnetic fields (*H* in kOe) (Rancourt and Ping, 1991) for NS goethite (Murad, 1982; Jang et al., 2003) and for hydrated hematite (Jang et al., 2007b). NS goethite showed master class *H* value at 330 kOe and hydrated hematite at 430 kOe (Figs. 5b′ and d′). NS magnetite was also identified, with significant deviation from the ideal ratio of tetrahedral and octahedral sites and deficient in Fe^{2+} (Murad and Schwertmann, 1993). Thermodynamic analysis indicated supersaturation for the stoichiometric magnetite that was not detected by MBS. Hence, we speculate that this NS magnetite might have been a solid solution of Fe(II) and Fe(III) (Génin et al., 2001) that controlled the observed $[Fe(II)_{diss}]$ during the reduction (Fig. 3). The formation of goethite from HFO is consistent with the literature, i.e., Fe(II) accelerates dissolution and re-precipitation reactions that result in dominance of goethite (Feitknecht and Michaelis, 1962; Pedersen et al., 2005).

4. Conclusions

1. The extents of Fe(II)-driven U(VI) reduction in the presence of HFO and hematite were similar, despite of large difference in the thermodynamic solubilities (hence, reduction potentials) of HFO and hematite.
2. During the reduction, extensive transformation of HFO and hematite was observed: goethite, hematite, and NS magnetite were formed from HFO; HFO, hydrated hematite, and NS magnetite were formed from hematite.
3. Based on measured aqueous [Fe(II)] and [U(VI)] plus assumed presence of amorphous uraninite, thermodynamic analysis indicated that $\{Fe^{3+}\}$ was controlled by HFO for both HFO and hematite experiments, which is consistent with solid products identified by MBS.
4. The Fe(II)/U(VI) reaction was retarded when high sorption density of U(VI) was applied for both HFO and hematite, suggesting that the reduction requires propinquity of reactive surface sites at which oxidation and reduction can occur.
5. The temporary increases in total U(VI) were observed, which is consistent with earlier research demonstrating meta-stability of sorbed U(V) species as well as changing redox potential due to phase changes in Fe(III) and U(IV) solids.

Acknowledgment

This research was supported by the Office of Science (BER), US Department of Energy, Grant no. DE-FG02-01-04ER63914 and by the National Science Foundation under Grant no. BES-0523196.

REFERENCES

Allard, T., Menguy, N., Salomon, J., Calligaro, T., Weber, T., Calas, G., Benedetti, M.F., 2004. Revealing forms of iron in river-borne material from major tropical rivers of the Amazon Basin (Brazil). Geochim. Cosmochim. Acta 68 (14), 3079–3094.

Amonette, J.E., Workman, D.J., Kennedy, D.W., Fruchter, J.S., Gorby, Y.A., 2000. Dechlorination of carbon tetrachloride by Fe(II) associated with goethite. Environ. Sci. Technol. 34 (21), 4606–4613.

Appelo, C.A.J., Postma, D., 1993. Geochemistry, Groundwater and Pollution. A.A. Balkema, Rotterdam.

Cornell, R.M., Schwertmann, U., 1996. The Iron Oxides: Structure, Properties, Reactions, Occurrence and Uses. VCH Publisher, New York.

Feitknecht, W., Michaelis, W., 1962. Uber die Hydrolyse von Eisen(III)-perchlorat-Losungen. Helv. Chim. Acta 45, 212–224.
Génin, J.-M.R., Refait, P., Bourrié, G., Abdelmoula, M., Trolard, F., 2001. Structure and stability of the Fe(II)–Fe(III) green rust "fougerite" mineral and its potential for reducing pollutants in soil solutions. Appl. Geochem. 16, 559–570.
Grenthe, I., Stumm, W., Laaksuharju, M., Nilsson, A.-C., Wikberg, P., 1992. Redox potentials and redox reactions in deep groundwater systems. Chem. Geol. 98, 131–150.
Gu, B., Liang, L., Dickey, M.J., Yin, X., Dai, S., 1998. Reductive precipitation of uranium(VI) by zero-valent iron. Environ. Sci. Technol. 32 (21), 3366–3373.
Gustafsson, J.P., 2006. Visual MINTEQ 2.50 〈http://www.lwr.kth.se/english/OurSoftware/vminteq/index.htm〉.
Ho, C.H., Miller, N.H., 1985. Effect of humic acid on uranium uptake by hematite particles. J. Colloid Interface Sci. 106 (2), 281–288.
Hobson, M.C.J., Gager, H.M., 1970. A Mössbauer effect study on crystallites of supported ferric oxide. J. Catal. 16, 254–263.
Ilton, E.S., Haiduc, A., Cahill, C.L., Felmy, A.R., 2005. Mica surfaces stabilize pentavalent uranium. Inorg. Chem. 44 (9), 2986–2988.
Jang, J.-H., Dempsey, B.A., Catchen, G.L., Burgos, W.D., 2003. Effects of Zn(II), Cu(II), Mn(II), Fe(II), NO_3^-, or SO_4^{2-} at pH 6.5 and 8.5 on transformations of hydrous ferric oxide (HFO) as evidenced by Mössbauer spectroscopy. Colloids Surf. A: Physicochemi. Eng. Aspects 221 (1–3), 55–68.
Jang, J.-H., Dempsey, B.A., Burgos, W.D., 2006. Solubility of schoepite: comparison and selection of complexation constants for U(VI). Water Res. 40 (14), 2738–2746.
Jang, J.-H., Dempsey, B.A., Burgos, W.D., 2007a. A model-based evaluation of sorptive reactivities of hydrous ferric oxide and hematite for U(VI). Environ. Sci. Technol. 41 (12), 4305–4310.
Jang, J.-H., Dempsey, B.A., Burgos, W.D., 2007b. Solubility of hematite revisited: effects of hydration. Environ. Sci. Technol. 41 (21), 7303–7308.
Lagarec, K., Rancourt, D.G., 1998. Recoil: Mössbauer Spectral Analysis Software for Windows, version 1.0.
Langmuir, D., 1978. Uranium solution-mineral equilibria at low temperatures with applications to sedimentary ore deposits. Geochim. Cosmochim. Acta 42, 547–569.
Langmuir, D., Whittemore, D.O., 1971. Variation in the stability of precipitated ferric oxyhydroxides. In: Gould, R.F. (Ed.), Nonequilibrium Systems in Natural Water Chemistry, pp. 209–234.
Larese-Casanova, P., Scherer, M.M., 2007. Fe(II) sorption on hematite: new insights based on spectroscopic measurements. Environ. Sci. Technol. 41 (2), 471–477.
Lenhart, J.J., Honeyman, B.D., 1999. Uranium(VI) sorption to hematite in the presence of humic acid. Geochim. Cosmochim. Acta 63 (19/20), 2891–2901.
Liger, E., Charlet, L., van Cappellen, P., 1999. Surface catalysis of uranium(VI) reduction by iron(II). Geochim. Cosmochim. Acta 63 (19/20), 2939–2955.
Lindberg, R.D., Runnells, D.D., 1984. Ground water redox reactions: an analysis of equilibrium state applied to Eh measurements and geochemical modeling. Science 225 (4665), 925–927.
Macalady, D.L., Langmuir, D., Grundl, T., Elzerman, A., 1990. Use of model-generated Fe^{3+} ion activities to compute Eh and ferric oxyhydroxide solubilities in anaerobic systems. In: Melchior, D.C., Bassett, R.L. (Eds.), Chemical Modeling of Aqueous Systems II. American Chemical Society, Washington, DC, pp. 350–367.
Missana, T., Maffiotte, C., Garcia-Gutierrez, M., 2003. Surface reactions kinetics between nanocrystalline magnetite and uranyl. J. Colloid Interface Sci. 261 (1), 154–160.
Morris, J.C., Stumm, W., 1967. Redox equilibria and measurements of potentials in the aquatic environment. In: Equilibrium Concepts in Natural Water Systems. American Chemical Society, Washington, DC, pp. 270–285.
Murad, E., 1982. The characterization of goethite by Mössbauer spectroscopy. Am. Mineral. 67 (9–10), 1007–1011.
Murad, E., 1990. Application of ^{57}Fe Mössbauer spectroscopy to problems in clay mineralogy and soil science: possibilities and limitations. Adv. Soil Sci. 12, 125–157.
Murad, E., Schwertmann, U., 1993. Temporal stability of a fine-grained magnetite. Clays Clay Miner. 41 (1), 111–113.
NIST, 2004. NIST Critically Selected Stability Constants of Metal Complexes Database. US Department of Commerce.
Park, B., Dempsey, B.A., 2005. Heterogeneous oxidation of Fe(II) on ferric oxide at neutral pH and a low partial pressure of O_2. Environ. Sci. Technol. 39 (17), 6494–6500.
Payne, T.E., Davis, J.A., Waite, T.D., 1996. Uranium adsorption on ferrihydrite—Effects of phosphate and humic acid. Radiochim. Acta 74, 239–243.
Pedersen, H.D., Postma, D., Jakobsen, R., Larsen, O., 2005. Fast transformation of iron oxyhydroxides by the catalytic action of aqueous Fe(II). Geochim. Cosmochim. Acta 69 (16), 3967–3977.
Petruzzelli, L., Celi, L., Ajmone-Marsan, F., 2005. Effects of soil organic fractions on iron oxide biodissolution under anaerobic conditions. Soil Sci. 170 (2), 102–109.
Postma, D., Appelo, C.A.J., 2000. Reduction of Mn-oxides by ferrous iron in a flow system: column experiment and reactive transport modeling. Geochim. Cosmochim. Acta 64 (7), 1237–1247.
Rancourt, D.G., Ping, J.Y., 1991. Voigt-based methods for arbitrary-shape static hyperfine parameter distributions in Mössbauer spectroscopy. Nucl. Instrum. Methods Phys Res. B: Beam Interact Mater. Atoms 58 (1), 85–97.
Renshaw, J.C., Butchins, L.J.C., Livens, F.R., May, I., Charnock, J.M., Lloyd, J.R., 2005. Bioreduction of uranium: environmental implications of a pentavalent intermediate. Environ. Sci. Technol. 39 (15), 5657–5660.
Schwertmann, U., 1966. Inhibitory effect of soil organic matter on the crystallization of amorphous ferric hydroxide. Nature 212 (5062), 645–646.
Silvester, E., Charlet, L., Tournassat, C., Gehin, A., Greneche, J.-M., Liger, E., 2005. Redox potential measurements and Mossbauer spectrometry of Fe^{II} adsorbed onto Fe^{III} (oxyhydr)oxides. Geochim. Cosmochim. Acta 69 (20), 4801–4815.
Sowder, A.G., Clark, S.B., Fjeld, R.A., 1998. The effect of sample matrix quenching on the measurement of trace uranium concentrations in aqueous solutions using kinetic phosphorimetry. J. Radioanalytical Nucl. Chem. 234 (1–2), 257–260.
Stauder, S., Raue, B., Sacher, F., 2005. Thioarsenates in sulfidic waters. Environ. Sci. Technol. 39 (16), 5933–5939.
Stumm, W., 1992. Chemistry of the Solid–Water Interface. Wiley, New York.
Stumm, W., Morgan, J.J., 1996. Aquatic Chemistry, third ed. Wiley, New York.
Tamura, H., Goto, K., Yotsuyanagi, T., Nagayama, M., 1974. Spectrophotometric determination of iron(II) with 1,10-phenanthroline in the presence of large amounts of iron(III). Talanta 21, 314–318.
Tamura, H., Goto, K., Nagayama, M., 1976. Effect of anions on the oxygenation of ferrous ion in neutral solutions. J. Inorganic Nucl. Chem. 38, 113–117.
Tipping, E., 1981. The adsorption of aquatic humic substances by iron oxides. Geochim. Cosmochim. Acta- 45 (2), 191–199.
Tipping, E., Rey-Castro, C., Bryan, S.E., Hamilton-Taylor, J., 2002. Al(III) and Fe(III) binding by humic substances in freshwaters, and implications for trace metal speciation. Geochim. Cosmochim. Acta 66 (18), 3211–3224.
Tronc, E., Belleville, P., Jolivet, J.-P., Livage, J., 1992. Transformation of ferric hydroxide into spinel by Fe^{II} adsorption. Langmuir 8 (1), 313–319.

Voelker, B.M., Morel, F.M.M., Sulzberger, B., 1997. Iron redox cycling in surface waters: effects of humic substances and light. Environ. Sci. Technol. 31 (4), 1004–1011.

Weber, T., Allard, T., Tipping, E., Benedetti, M.F., 2006. Modeling iron binding to organic matter. Environ. Sci. Technol. 40 (24), 7488–7493.

Wehrli, B., Sulzberger, B., Stumm, W., 1989. Redox processes catalyzed by hydrous oxide surfaces. Chem. Geol. 78, 167–179.

Williams, A.G.B., Scherer, M.M., 2004. Spectroscopic evidence for Fe(II)–Fe(III) electron transfer at the iron oxide–water interface. Environ. Sci. Technol. 38 (18), 4782–4790.